Journal of Materials Chemistry C

RSC Publishing

PAPER

View Article Online
View Journal | View Issue

Cite this: J. Mater. Chem. C, 2013, 1, 2368

Facile synthesis and characterization of iridium(III) complexes containing an *N*-ethylcarbazole–thiazole main ligand using a tandem reaction for solution processed phosphorescent organic light-emitting diodes†

Thota Giridhar,[a] Woosum Cho,[a] Juhyeon Park,[a] Jin-Su Park,[a] Yeong-Soon Gal,[b] Sunwoo Kang,[c] Jin Yong Lee[c] and Sung-Ho Jin*[a]

Received 3rd October 2012
Accepted 29th January 2013

DOI: 10.1039/c3tc00323j

www.rsc.org/MaterialsC

A new series of highly efficient phosphorescent Ir(III) complexes, which have potential applications in solution processable phosphorescent organic light-emitting diodes (PhOLEDs), were synthesized and their photophysical, electrochemical, and electroluminescent (EL) properties were investigated. The Ir(III) complexes, including (Et-Cz–Tz)$_2$Ir(pic), (Et-Cz–Tz)$_2$Ir(pic-*N*-O), (Et-Cz–Tz)$_2$Ir(EO$_2$–pic), and (Et-Cz–Tz)$_2$Ir(EO$_2$–pic-*N*-O), are comprised of linked *N*-ethylcarbazole (Et-Cz) and thiazole (Tz) units as the main ligand (Et-Cz–Tz) and picolinic acid (pic) and picolinic acid *N*-oxide (pic-*N*-O) as ancillary ligands. In addition, some of the Ir(III) complexes contain an ethylene oxide solubilizing group attached to the ancillary ligands *via* a tandem reaction. High performance, solution processable PhOLEDs, fabricated using (Et-Cz–Tz)$_2$Ir(EO$_2$–pic), were observed to have a maximum external quantum efficiency of 6.08% and a luminance efficiency of 10.98 cd A^{-1}. This is the first report on the use of EO$_2$–pic and EO$_2$–pic-*N*-O ancillary ligands for the synthesis of solution processable Ir(III) complexes *via* a tandem reaction. The performances of the PhOLEDs based on these Ir(III) complexes correlate well with the theoretical properties predicted by using density functional theory calculations.

Introduction

Much interest exists currently in organic light-emitting diodes (OLEDs) that can be employed in full color display and lighting applications.[1,2] Fluorescence emitting materials used in these devices make use of only singlet excitons and, thus, their theoretical maximum light emission efficiency is 25%. However, phosphorescent emitting materials have significantly improved OLED performance because both singlet and triplet excitons can participate in light emission.[3,4] Owing to their high efficiencies and facile color tunabilities, compared with those of other metal–ligand complexes like those derived from ruthenium,[5–7] osmium,[8–10] and copper,[11] Ir(III) complexes have become the most popular photoluminescent (PL) dopant materials.[12–14]

The development of yellow emitting Ir(III) complexes is an important goal of efforts aimed at producing white OLEDs (WOLEDs) and full-color displays, which rely on the use of mixtures of either the three primary colors (red, green and blue) or two complementary colors (*e.g.*, blue and yellow).[15–17] In a recent investigation, we synthesized highly efficient, red emitting Ir(III) complexes that are comprised of *N*-ethylcarbazole (Et-Cz)-containing phenylquinoline (Et-Cz–PhQ) moieties as a main ligand along with picolinic acid (pic) and picolinic acid *N*-oxide (pic-*N*-O) as ancillary ligands.[18]

Our interest in carbazoles (Cz) and thiazole (Tz) as main ligands in Ir(III) complexes was stimulated by the fact that derivatives of these substances have unique hole or electron-transporting properties, and by the thought that these properties might play important roles in improving the performances of electroluminescent (EL) materials.[19–25] Cz-based materials have unique optical, electronic and chemical properties, exemplified by their light absorption in the near UV region and low redox potentials. Moreover, the Cz backbone is readily functionalized at the 3-, 6-, 9-positions and, as a result, it can be covalently linked to other important groups. Furthermore, in comparison to thiophene, the Tz ring system contains an sp^2-hybridized nitrogen in place of carbon, which makes it more electron deficient. This feature might assist emission

[a]Department of Chemistry Education, Graduate Department of Frontier Materials Chemistry, Institute for Plastic Information and Energy Materials, Pusan National University, Busan, 609-735, Republic of Korea. E-mail: shjin@pusan.ac.kr; Fax: +82-51-581-2348; Tel: +82-51-510-2727

[b]Polymer Chemistry Lab, College of General Education, Kyungil University, Hayang, 712-701, Republic of Korea

[c]Department of Chemistry, Sungkyunkwan University, Suwon, 440-746, Republic of Korea

† Electronic supplementary information (ESI) available. See DOI: 10.1039/c3tc00323j

wavelength tuning of Ir(III) complexes through the incorporation of a main ligand that incorporates both the Et-Cz and Tz groups.

Multistep processes carried out using one synthetic operation are known as tandem reactions.[26,27] The reactions not only construct complex structures in a single step but they also eliminate isolation and purification steps. A number of solution processable Ir(III) complexes have been prepared using multiple-step synthetic procedures. However no reports exist about the synthesis of solution processable small molecules based on Ir(III) complexes *via* tandem processes.

In most applications, small molecule-based phosphorescent OLEDs (PhOLEDs) are prepared by using thermal high vacuum evaporation technologies to deposit up to six organic layers. Devices made in this manner perform better than their solution-processed PhOLED counterparts.[1,28] However, the use of thermal evaporation deposition makes the fabrication process relatively complicated and involves limited utilization of the expensive materials.[29–31] Recently, solution processing technologies, such as spin-coating and inkjet printing, represent good alternatives for PhOLED fabrication because of their ready scalability and cost competitiveness. Recently, much attention in the area of solution-processed PhOLEDs has been given to the design and preparation of suitable small molecules and to the optimization of device architectures. The majority of solution processed PhOLEDs based on Ir(III) complexes are composed of layers that contain oligomers or conjugated polymers,[32,33] and more recently dendrimers.[34,35] Disadvantages associated with the use of these types of materials include the fact that methods requiring multistep reaction sequences are needed for the synthesis of intermediates or the Ir(III) complexes and that it is difficult to generate high purity Ir(III) complexes. Recently, solution processable small molecules, which combine the advantageous features of both polymeric and small molecule materials, have been developed. For this purpose, the design of novel solution processable Ir(III) complexes and their

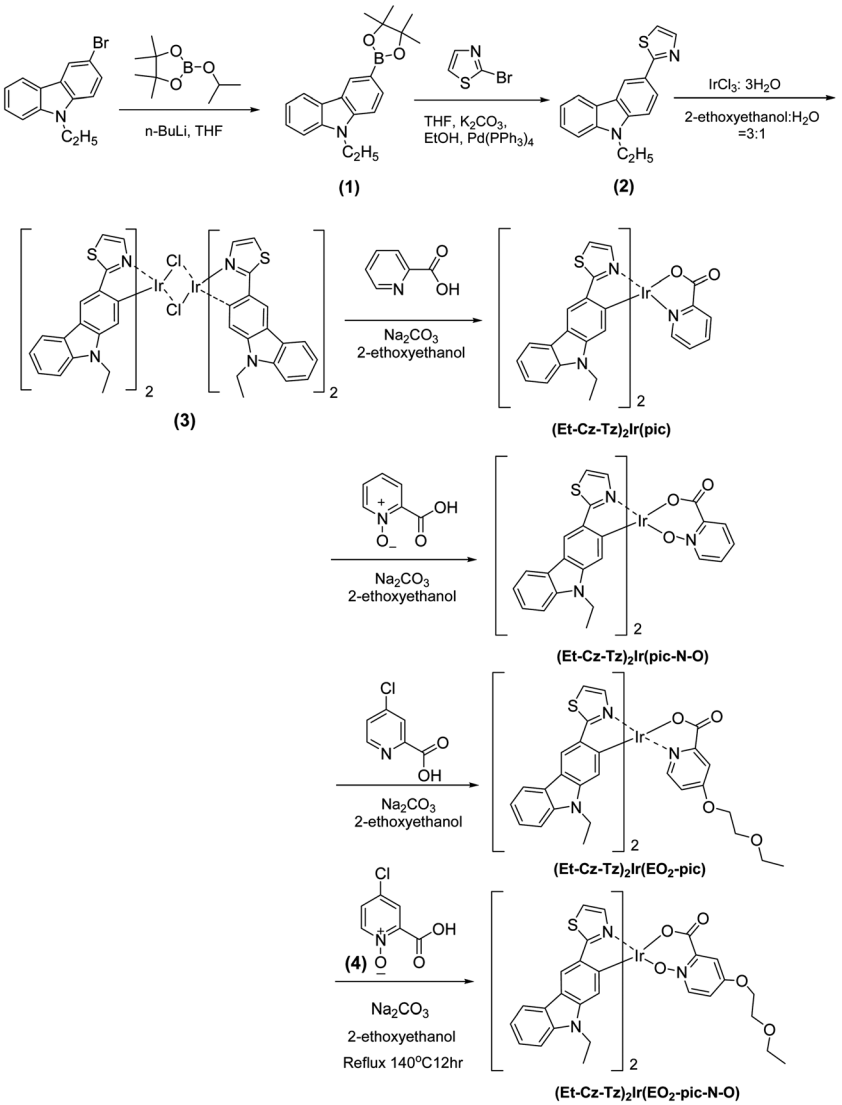

Scheme 1 Routes for the synthesis of Ir(III) complexes.

synthesis using tandem reaction sequences is of great importance.

In the studies described below, we have designed and synthesized selected members of a new series of solution processable greenish-yellow Ir(III) complexes that contain 2-(9-ethyl-9*H*-carbazol-3-yl)thiazole (Et-Cz–Tz) as a main ligand and ancillary ligands comprised of either picolinic acid or picolinic acid *N*-oxide or 4-chloropicolinic acid or 4-chloropicolinic acid *N*-oxide, the latter of which contains a functionality that enables the introduction of the solubilizing, electron donating ethylene oxide (EO) group. The methodology involved in the preparative routes employs tandem reactions,[30,31] which enable the construction of complex structures in single step processes that do not require isolation and purification of synthetic intermediates.

The strategy used to design new Ir(III) complexes incorporates several features. Because Ir(III) complexes have been compatible with both solution process and vacuum deposition methodologies for PhOLED fabrication, as mentioned above, the Ir(III) complexes should incorporate an ambipolar type main ligand that is comprised of a combination of *N*-ethylcarbazole (Et-Cz) as a p-type and Tz as an n-type semiconductor to bring about synergic effects on hole and electron-transporting properties. The picolinic acid derivatives or corresponding *N*-oxides would serve as ancillary ligands and as sites to which groups that enhance the solubility of the Ir(III) complexes could be attached. The four Ir(III) complexes, (Et-Cz–Tz)$_2$Ir(pic), (Et-Cz–Tz)$_2$Ir(pic-*N*-O), (Et-Cz–Tz)$_2$Ir(EO$_2$–pic), and (Et-Cz–Tz)$_2$Ir(EO$_2$–pic-*N*-O) (Scheme 1), which contain these features, were selected for the studies described below.

Results and discussion

The first phase of this investigation focused on Et-Cz–Tz (**2**, Scheme 1), which we proposed would be an ideal main ligand for greenish-yellow emitting Ir(III) complexes. Synthesis of **2** began with Suzuki coupling reaction of 9-ethyl-3-(4,4,5,5-tetramethyl-1,3,2-dioxaborolan-2-yl)-9*H*-carbazole (**1**) with 2-bromothiazole, which formed the desired donor–acceptor type of Et-Cz–Tz ligand in 76% yield. The cyclometalated Ir(III) μ-chloride bridged dimer **3** was then generated by reaction of iridium trichloride hydrate with an excess quantity of the main ligand **2**. Four heteroleptic Ir(III) complexes shown in Scheme 1 were then produced by reaction of **3** with four ancillary ligands, including picolinic acid (pic), picolinic acid *N*-oxide (pic-*N*-O), 4-chloropicolinic acid and 4-chloropicolinic acid *N*-oxide. The generated Ir(III) complexes, (Et-Cz–Tz)$_2$Ir(pic), (Et-Cz–Tz)$_2$Ir(pic-*N*-O), (Et-Cz–Tz)$_2$Ir(EO$_2$–pic), and (Et-Cz–Tz)$_2$Ir(EO$_2$–pic-*N*-O), were purified using silica column chromatography and their structures and purities were determined using ^{1}H-, ^{13}C-NMR, elemental analysis, HPLC, HR-MS, differential scanning calorimetry (DSC), thermal gravimetric analysis (TGA), cyclic voltammetry (CV), UV-visible absorption spectroscopy, PL spectroscopy, and computational methods.

There are two possible sites for cyclometalation at the 2nd and 4th positions of the carbazole unit by using 2-(9-ethyl-9*H*-carbazol-3-yl)thiazole as a main ligand.[25] The possibility of forming an Ir metal bond at the 2nd position of the carbazole unit was confirmed by 600 MHz ^{1}H-NMR spectroscopy. The ^{1}H-NMR spectrum of (Et-Cz–Tz)$_2$Ir(pic-*N*-O) clearly showed four singlet proton peaks at 8.27, 8.25, 6.29, and 6.21 ppm. If the Ir metal bond is linked at the 4th position of the carbazole unit, there is no chance of getting four singlet proton peaks. The other proton signal positions and the number from the peak integrations are consistent with the proposed chemical structure of the Ir(III) complexes.

The bands at 2910 and 2400 cm^{-1} indicate the presence of an alkyl group and an ammonium ion, as shown in Fig. S1.† A carbonyl group (C=O) and a carboxylic ester (C–O) of picolinic acid derivatives were found at 1660 and 1240 cm^{-1}, respectively. All four synthesized iridium(III) complexes have these functional groups (Fig. 1).

Among the four heteroleptic Ir(III) complexes, (Et-Cz–Tz)$_2$Ir(pic) and (Et-Cz–Tz)$_2$Ir(pic-*N*-O) were purified by the train sublimation method before device fabrication. The purity of (Et-Cz–Tz)$_2$Ir(pic) and (Et-Cz–Tz)$_2$Ir(pic-*N*-O) thus obtained was confirmed to be >99.0% by HPLC analysis. Due to the introduction of the ethylene oxide as a solubilizing group into ancillary ligands, it was observed that (Et-Cz–Tz)$_2$Ir(EO$_2$–pic) and (Et-Cz–Tz)$_2$Ir(EO$_2$–pic-*N*-O) were decomposed during sublimation. The thermal properties of the Ir(III) complexes under a N_2 atmosphere were evaluated using TGA and DSC. The 5% weight loss temperatures ($\Delta T_{5\%}$) of the Ir(III) complexes are given in Fig. 2 and summarized in Table 1. The TGA data reveal that the $\Delta T_{5\%}$ of (Et-Cz–Tz)$_2$Ir(pic), (Et-Cz–Tz)$_2$Ir(pic-*N*-O), (Et-Cz–Tz)$_2$Ir(EO$_2$–pic), and (Et-Cz–Tz)$_2$Ir(EO$_2$–pic-*N*-O) are 344, 336, 340, and 330 °C, respectively. The Ir(III) complexes with pic ancillary ligands have relatively higher $\Delta T_{5\%}$ values than those containing the pic-*N*-O ancillary ligands. The thermal stabilities of Ir(III) complexes with ethylene oxide linked to the pic and pic-*N*-O moieties are nearly identical to those of the Ir(III) complexes with pic and pic-*N*-O ancillary ligands. The glass transition temperatures (T_g) of Ir(III) complexes were found to be in the range of 212–254 °C. Thus, it appears that the rigidity of the Ir(III) complexes will prevent degradation of the emitting layer by the current-induced heat caused by the operation of PhOLEDs.

The absorption spectra of the Ir(III) complexes and the main ligand, Et-Cz–Tz, in chloroform solution are displayed in Fig. 3(a). The photophysical properties of the Ir(III) complexes are summarized in Table 1. As with most Ir(III) complexes, the absorption spectra can be divided into two regions.[36,37] The intense peak in the short wavelength region below 360 nm in each spectrum is assigned to a spin-allowed $^1\pi$–π^* transition, which closely resembles the corresponding transition in Et-Cz–Tz (λ_{max}: 330 nm). The weaker absorption tail that appears above 360 nm is due to a charge transfer transition.[38] The data suggest that substantial mixing occurs between the ligand-based $^3\pi$–π^* states, spin forbidden metal to ligand charge transfer (^{3}MLCT) and higher-lying ^{1}MLCT transition induced by the spin–orbit coupling effect.[39] Spin–orbit coupling is enhanced by the presence of both closely spaced π–π^* and MLCT states and the heavy-atom effect of iridium metal.[40] The optical band gaps (E_g^{opt}) of all Ir(III) complexes were determined from the UV-visible absorption edge to be 2.60 eV.

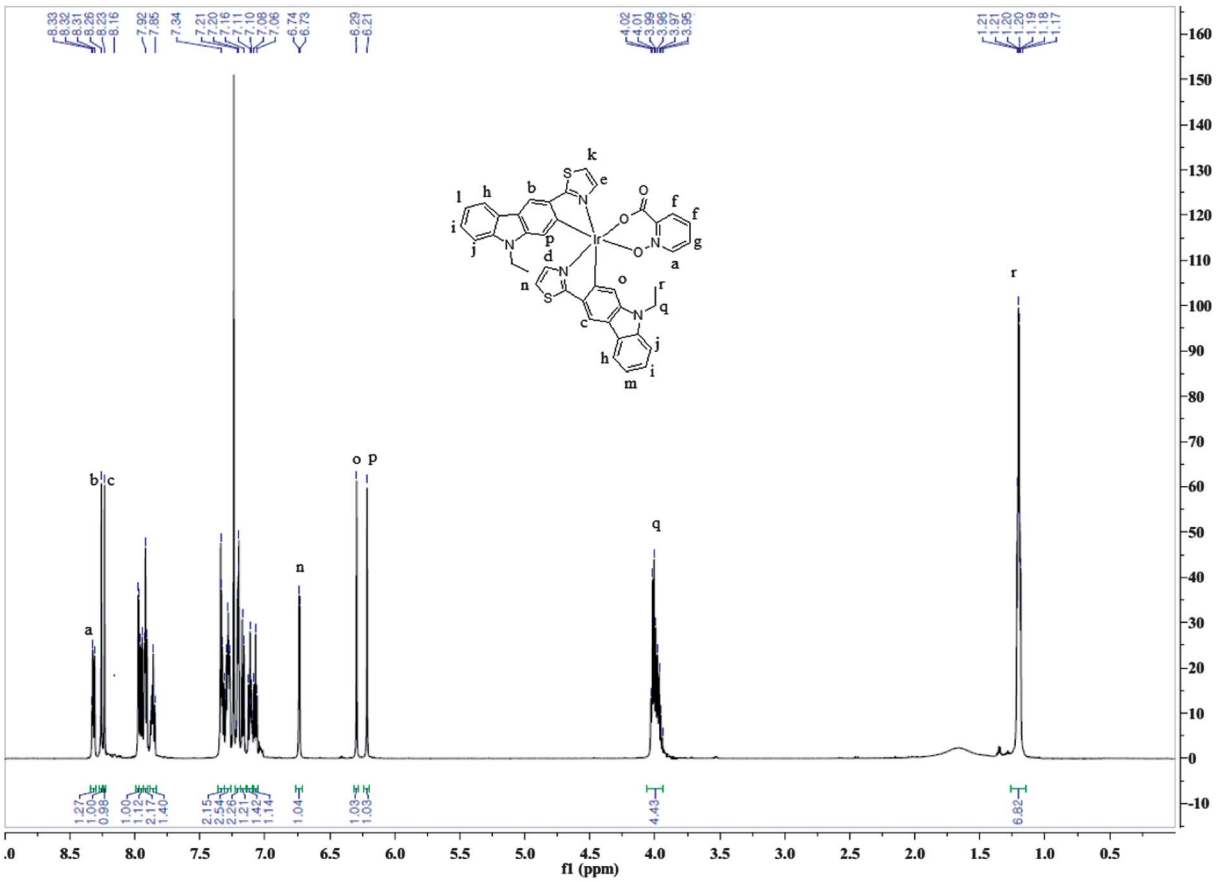

Fig. 1 ^{1}H-NMR spectrum (600 MHz, 298 K, $CDCl_3$) of (Et-Cz–Tz)$_2$Ir(pic-*N*-O).

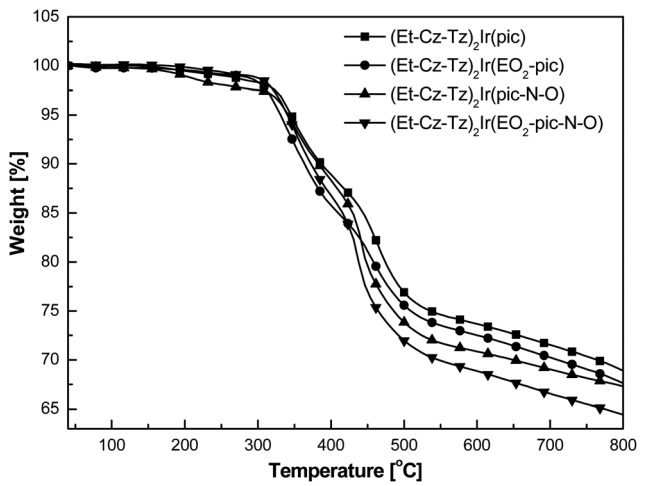

Fig. 2 TGA trace of (Et-Cz–Tz)$_2$Ir(pic), (Et-Cz–Tz)$_2$Ir(pic-*N*-O), (Et-Cz–Tz)$_2$Ir(EO_2–pic), and (Et-Cz–Tz)$_2$Ir(EO_2–pic-*N*-O) measured at a scan rate of 10 °C min^{-1} under a N_2 atmosphere.

Under photoexcitation, all Ir(III) complexes emit intense greenish-yellow light (PL spectra in Fig. 3(b)). Maximum emission peaks of thin film PL spectra of the Ir(III) complexes, independent of whether they do or do not contain an ethylene oxide unit on the pic and pic-*N*-O ancillary ligands, are nearly identical to those of the solution PL spectra. On the other hand, a small red-shift from solution to film for Ir(III) complexes was observed, which may be related to a slight aggregate formation and/or intermolecular interactions between the Ir(III) complexes. The findings show that the ethylene oxide unit does not alter the optical properties of Ir(III) complexes and, thus, that its only role would be to increase the solubility of the Ir(III) complex and to aid in the fabrication of solution processed PhOLEDs. The photoluminescence quantum yields (Φ_{pl}) of the Ir(III) complexes in toluene solution were determined using Ir(ppy)$_3$ as an actinometer (Φ_{pl} = 0.4).[41,42] The Φ_{pl} for (Et-Cz–Tz)$_2$Ir(pic), (Et-Cz–Tz)$_2$Ir(pic-*N*-O), (Et-Cz–Tz)$_2$Ir(EO_2–pic), and (Et-Cz–Tz)$_2$Ir(EO_2–pic-*N*-O) were found to be in the range of 0.11–0.13.

To investigate the charge carrier injection properties of the Ir(III) complexes and to evaluate the energies of their highest occupied molecular orbitals (HOMO) and lowest unoccupied molecular orbitals (LUMO), the electrochemical properties of the Ir(III) complexes were determined by using CV. All Ir(III) complexes display irreversible redox waves over both the anodic and cathodic ranges. The onset oxidation potentials of the Ir(III) complexes are in the range of 0.7–0.8 V (Fig. 4), which corresponds to HOMO energy levels of −5.4 to −5.5 eV. The LUMO energy levels, calculated using the onset reduction potentials, were found to be *ca.* −2.8 to −2.9 eV for these Ir(III) complexes.

Table 1 Photophysical, electrochemical and thermal data for Ir(III) complexes

Compound	T_d[a] [°C]	T_g[b] [°C]	λ_{abs} [nm] (log ε)[c]	λ_{em}[d] [nm]	λ_{em}[e] [nm]	Φ_{pl}[f] [%]	HOMO/LUMO[g] [eV]
(Et-Cz–Tz)$_2$Ir(pic)	344	245	318(4.9), 386(4.5), 442(3.9)	537, 575	542, 580	0.132	−5.5/−2.9
(Et-Cz–Tz)$_2$Ir(EO$_2$–pic)	336	212	320(4.9), 387(4.6), 442(4.0)	537, 574	541, 580	0.115	−5.5/−2.9
(Et-Cz–Tz)$_2$Ir(pic-*N*-O)	340	254	320(4.9), 386(4.5), 442(3.9)	537, 576	541, 579	0.141	−5.4/−2.8
(Et-Cz–Tz)$_2$Ir(EO$_2$–pic-*N*-O)	330	225	318(4.9), 386(4.5), 444(4.0)	535, 574	542, 581	0.114	−5.4/−2.8

[a] Temperature with 5% mass loss measure by TGA with a heating rate of 10 °C min^{-1} under N_2. [b] Glass transition temperature, determined by DSC with a heating rate of 10 °C min^{-1} under N_2. [c] Measured in toluene solution at 1.0×10^{-5} M concentration. [d] Maximum emission wavelength, measured in toluene solution at 1.0×10^{-5} M. [e] Maximum emission wavelength, measured in a film state. [f] Measured in 1×10^{-5} M toluene solution relative to Ir(ppy)$_3$ ($\Phi_{pl} = 0.4$) with 381 nm excitation. [g] Determined from the onset of CV oxidation and reduction.

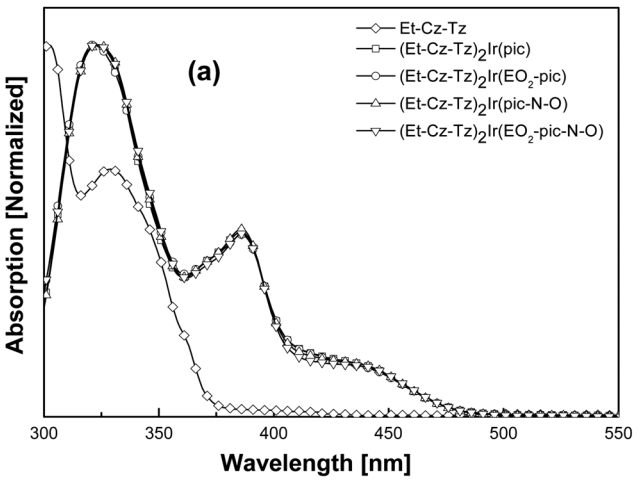

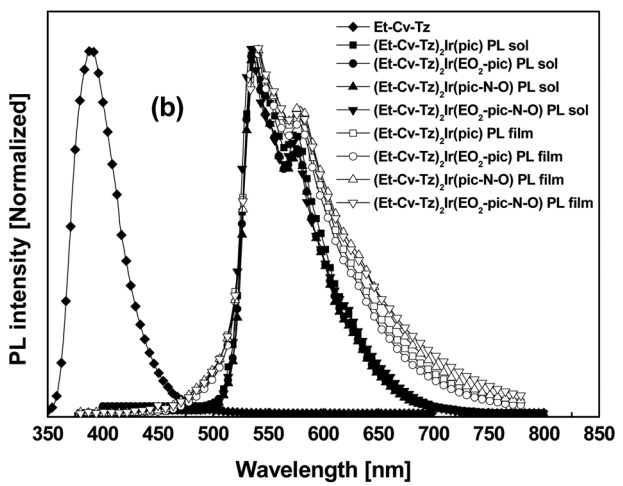

Fig. 3 UV-visible absorption (a) and PL (b) spectra of Et-Cz–Tz and Ir(III) complexes in $CHCl_3$ at 25 °C.

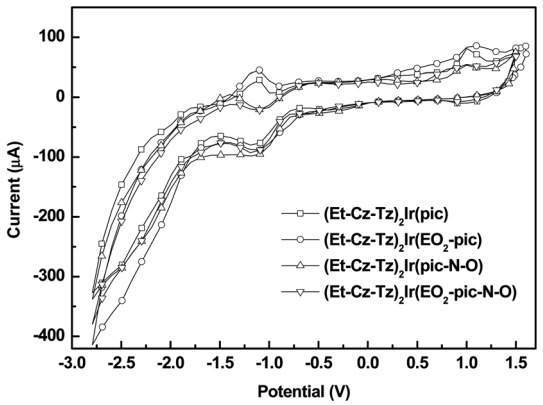

Fig. 4 Cyclic voltammograms of Ir(III) complexes in tetra-*n*-butylammonium hexafluorophosphate ($TBAPF_6$) at a scan rate of 100 mV s^{-1}.

The electrochemical band gaps (E_g^{EC}) of the Ir(III) complexes (Fig. 4 and Table 1) were calculated to be 2.6 eV.

To evaluate the EL properties of the Ir(III) complexes, typical PhOLEDs were fabricated using (Et-Cz–Tz)$_2$Ir(pic), (Et-Cz–Tz)$_2$Ir(pic-*N*-O), (Et-Cz–Tz)$_2$Ir(EO$_2$–pic), and (Et-Cz–Tz)$_2$Ir(EO$_2$–pic-*N*-O) as dopants in the emission layer. The PhOLEDs consisted of multilayer films with a configuration of ITO/PEDOT:PSS (40 nm)/*m*-MTDATA:TPBI:Ir(III) complexes (50 nm)/TPBI (20 nm)/LiF (1 nm)/Al (100 nm). 4,4′,4″-Tris[3-methylphenyl(phenyl)amino]triphenylamine (*m*-MTDATA) and 1,3,5-tri(1-phenyl-1*H*-benzo[*d*]imidazol-2-yl)phenyl (TPBI) served as hosts for Ir(III) complexes and an additional TPBI as a hole blocking, and electron transporting layers were inserted between the emitting layer and the LiF:Al cathode. Prior to deposition of the organic layer, the ITO substrates were exposed to UV-ozone flux for 10 min and then degreased in acetone and isopropyl alcohol. In order to investigate the effect of Ir(III) complexes on performance, PhOLEDs were fabricated with variable concentration (10%, 12% and 14%) of Ir(III) complexes doped into *m*-MTDATA : TPBI (2 : 1) as an emission layer and were spin-coated with chlorobenzene to give 50 nm thick films. The organic layers were then deposited by using thermal evaporation at a base pressure of $<5 \times 10^{-6}$ Torr.

Solution processing is a simpler method for PhOLED fabrication. Thus, the emitting layers in the PhOLEDs can be prepared using the spin-coating method. The detailed device architecture and energy levels of each layer are shown in Fig. 5. The presence of solubilizing groups in the ancillary ligands gives the Ir(III) complexes an amorphous nature and good film forming properties and chemical compatibility with the *m*-MTDATA and TPBI hosts. Because their respective HOMO and LUMO energies match those of the Ir(III) complexes, hole injection is facilitated by *m*-MTDATA and electron injection is aided by the TPBI layer.

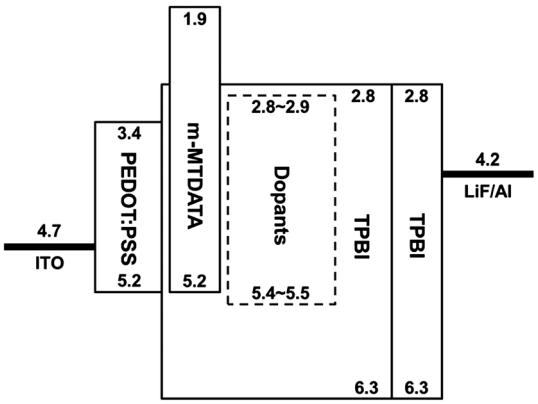

Fig. 5 The relative HOMO and LUMO energy diagram for the PhOLEDs.

The morphology of the emitting layer is very important in determining the efficiencies of solution processed PhOLEDs. Atomic force microscopy (AFM) was employed to investigate the morphology of the emitting layer composed of *m*-MTDATA : TPBI (2 : 1) doped with 12 wt% of Ir(III) complex blend films. Inspection of the AFM images (Fig. 6) of the emitting layers shows that they exhibit typical amorphous morphologies without any crystalline domains. The rms roughnesses of (Et-Cz–Tz)$_2$Ir(pic), (Et-Cz–Tz)$_2$Ir(EO$_2$–pic), (Et-Cz–Tz)$_2$Ir(pic-*N*-O), and (Et-Cz–Tz)$_2$Ir(EO$_2$–pic-*N*-O) are 0.511, 0.365, 0.467, and 0.341 nm, respectively. These findings suggest that (Et-Cz–Tz)$_2$Ir(EO$_2$–pic) and (Et-Cz–Tz)$_2$Ir(EO$_2$–pic-*N*-O) are uniformly dispersed compared to (Et-Cz–Tz)$_2$Ir(pic) and (Et-Cz–Tz)$_2$Ir(pic-*N*-O), owing to the presence of the ethylene oxide solubilizing group through solution processing with homogeneous dispersion. There was no phase separation or any aggregated domains.

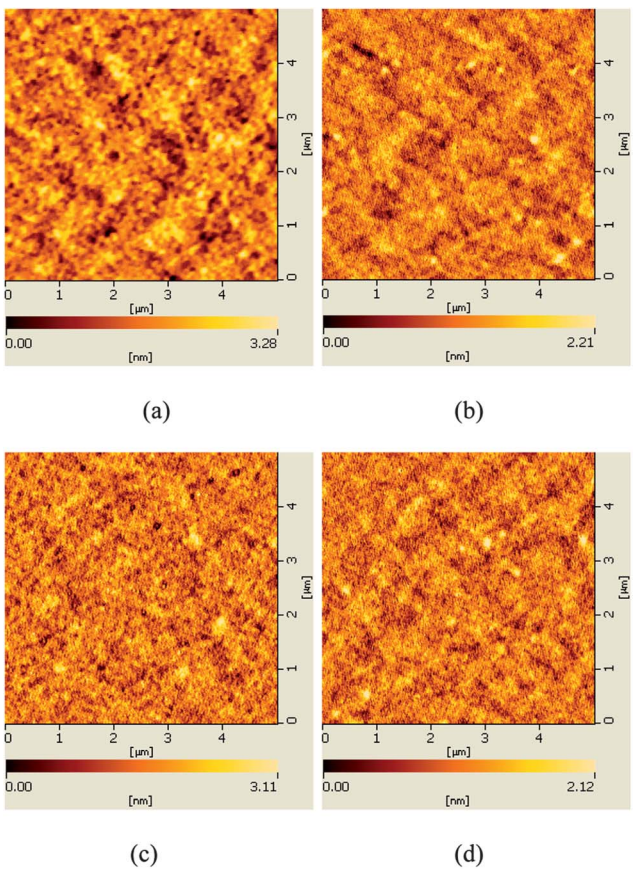

Fig. 6 AFM topographic images of 12 wt% of Ir(III) complexes doped into *m*-MTDATA : TPBI (2 : 1) as an emission layer. (Et-Cz–Tz)$_2$Ir(pic) (a), (Et-Cz–Tz)$_2$Ir(EO$_2$–pic) (b), (Et-Cz–Tz)$_2$Ir(pic-*N*-O) (c), and (Et-Cz–Tz)$_2$Ir(EO$_2$–pic-*N*-O) (d). The films were prepared through spin-coating from chlorobenzene solutions onto ITO/PEDOT:PSS.

EL spectra of Ir(III) complexes at a current density of 10 mA cm^{-2}, given in Fig. 7, contain greenish-yellow emission peaks with maxima at *ca.* 535 nm and shoulders at 580 nm. The fact that these features closely match those present in the corresponding PL spectra demonstrates that EL emission originates from the triplet excited states of the Ir(III) complexes arising from direct recombination of holes and electrons located within the emitting layer. The CIE coordinates of (Et-Cz–Tz)$_2$Ir(pic), (Et-Cz–Tz)$_2$Ir(pic-*N*-O), (Et-Cz–Tz)$_2$Ir(EO$_2$–pic), and (Et-Cz–Tz)$_2$Ir(EO$_2$–pic-*N*-O) were observed to be (0.44, 0.56), (0.44, 0.54), (0.43, 0.56), and (0.42, 0.55), respectively.

The current density–voltage–luminance (*J*–*V*–*L*) characteristics of PhOLEDs, comprised of different ancillary ligands with and without the ethylene oxide solubilizing group, are given in Fig. 8(a). The performances and EL emission characteristics of the PhOLEDs are summarized in Table 2. The maximum brightness of the PhOLEDs using (Et-Cz–Tz)$_2$Ir(pic), (Et-Cz–Tz)$_2$Ir(pic-*N*-O), (Et-Cz–Tz)$_2$Ir(EO$_2$–pic), and (Et-Cz–Tz)$_2$Ir(EO$_2$–pic-*N*-O) was found to be 2381, 2310, 1892, and 2450 cd m^{-2}, respectively. The turn-on voltages of the PhOLEDs are low (*ca.* 3.0 V), a phenomenon that is likely a result of the fact that *m*-MTDATA and the Ir(III) complexes have well matched HOMO energies and, consequently, a negligible barrier exists for injection of holes from the PEDOT:PSS layer. Fig. 8(b) displays plots of external quantum (EQE) and luminance efficiencies *versus* current densities of the PhOLEDs. The maximum EQEs of

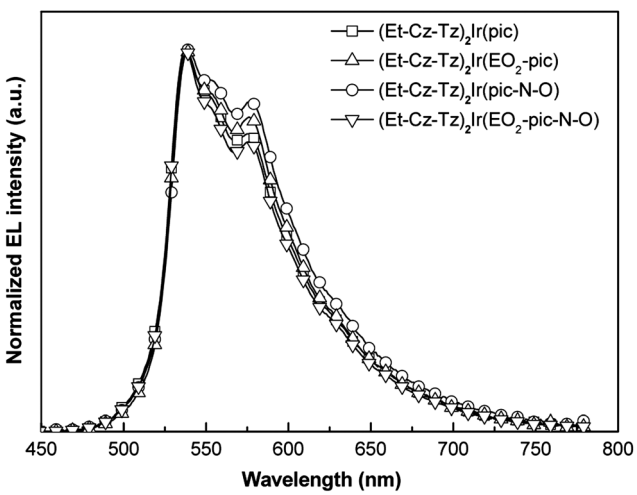

Fig. 7 EL spectra of the Ir(III) complexes.

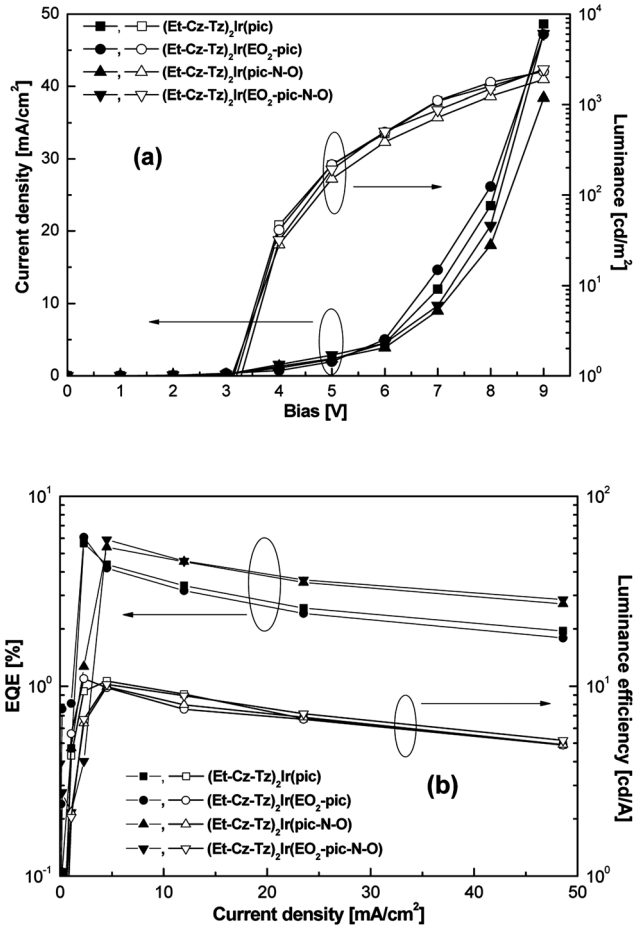

Fig. 8 Current density–voltage–luminance plots (a) and external quantum efficiency–current density–luminance efficiencies (b) for the PhOLEDs.

PhOLEDs comprised of (Et-Cz–Tz)$_2$Ir(pic), (Et-Cz–Tz)$_2$Ir(pic-*N*-O), (Et-Cz–Tz)$_2$Ir(EO$_2$–pic), and (Et-Cz–Tz)$_2$Ir(EO$_2$–pic-*N*-O) were found to be 5.64, 6.08, 5.39, and 5.91%, respectively. In addition, changes in the current density of (Et-Cz–Tz)$_2$Ir(EO$_2$–pic) based on PhOLEDs from 1 to 10 to 30 mA cm^{-2} cause respective decreases in EQE from 6.08% to 4.18% to 2.41%. The decrease of EQE with increasing current density is a consequence of increased triplet–triplet annihilation and field-induced quenching effects.[43]

To gain insight into the observed photo-physical properties of the phosphorescent Ir(III) complexes, density functional theory (DFT) calculations were carried out employing the nonlocal density functional of Becke's three parameterized Lee–Yang–Parr exchange functional (B3LYP) and a suite of Gaussian 09 programs.[44] Iridium metal was treated by employing a Hay–Wadt effective core potential of a double zeta basis set (LANL2DZ) and the 6-31G* basis set was employed to describe other atoms. It should be noted that in previous studies, the same calculation methods employed in the current effort led to reliable predictions of the photo-physical properties of Ir(III) complexes.[22] The results of the calculations show that ligands, such as Et-Cz–Tz and pic (or pic-*N*-O), are octahedrally coordinated to iridium with C–Ir distances of 2.022–2.038 Å and N–Ir distances of 2.031–2.188 Å in all of the Ir(III) complexes. The calculated highest energy occupied molecular orbitals (HOMOs) and lowest energy unoccupied molecular orbitals (LUMOs), which have similar shapes in all Ir(III) complexes, are shown in Fig. 9. Electron densities in the HOMOs of (Et-Cz–Tz)$_2$Ir(pic), (Et-Cz–Tz)$_2$Ir(pic-*N*-O), and (Et-Cz–Tz)$_2$Ir(EO$_2$–pic-*N*-O) are mainly distributed over the Et-Cz–Tz moiety and iridium metal, while the LUMOs are mostly distributed over the ancillary ligands (pic or pic-*N*-O). For the (Et-Cz–Tz)$_2$Ir(EO$_2$–pic) containing complex, electron density in the HOMO is mainly delocalized on one of the Et-Cz–Tz moieties, while the LUMO is distributed over the other Et-Cz–Tz moiety. Analysis of the shapes of HOMOs and LUMOs shows that MLCT (metal to ligand charge transfer) takes place from iridium to the Et-Cz–Tz moiety in the (Et-Cz–Tz)$_2$Ir(pic), (Et-Cz–Tz)$_2$Ir(pic-*N*-O), (Et-Cz–Tz)$_2$Ir(EO$_2$–pic) and (Et-Cz–Tz)$_2$Ir(EO$_2$–pic-*N*-O) complexes. Time-dependent DFT calculations with consideration of the solvent effect were performed on the optimized geometries in order to determine the theoretical UV-visible absorption properties of the Ir(III) complexes. The results show that the excitation energies of (Et-Cz–Tz)$_2$Ir(pic), (Et-Cz–Tz)$_2$Ir(EO$_2$–pic), (Et-Cz–Tz)$_2$Ir(pic-*N*-O), and (Et-Cz–Tz)$_2$Ir(EO$_2$–pic-*N*-O) are

Table 2 EL performance of PhOLEDs with solution processed emitting layers

Compound	Concentration [%]	Turn on[a] [V]	EQE[b] [%]	EQE[c] [%]	CE[b] [cd A]	PE[b] [lm W^{-1}]	Brightness[b] [cd m^{-2}]	CIE[d] (x,y)
(Et-Cz–Tz)$_2$Ir(pic)	10	3.33	3.99	2.83	7.78	2.89	2096	(0.43, 0.55)
(Et-Cz–Tz)$_2$Ir(EO$_2$–pic)	10	3.54	4.39	3.41	8.56	3.37	2322	(0.43, 0.55)
(Et-Cz–Tz)$_2$Ir(pic-*N*-O)	10	3.31	3.15	2.96	7.26	2.66	2240	(0.43, 0.55)
(Et-Cz–Tz)$_2$Ir(EO$_2$–pic-*N*-O)	10	3.31	4.13	3.03	8.46	3.17	2637	(0.43, 0.56)
(Et-Cz–Tz)$_2$Ir(pic)	12	3.15	5.64	2.12	10.65	5.90	2381	(0.44, 0.56)
(Et-Cz–Tz)$_2$Ir(EO$_2$–pic)	12	3.20	6.08	2.58	10.98	6.89	2310	(0.44, 0.54)
(Et-Cz–Tz)$_2$Ir(pic-*N*-O)	12	3.10	5.39	0.95	9.93	5.19	1892	(0.43, 0.56)
(Et-Cz–Tz)$_2$Ir(EO$_2$–pic-*N*-O)	12	3.30	5.91	0.35	10.22	5.87	2450	(0.42, 0.55)
(Et-Cz–Tz)$_2$Ir(pic)	14	3.56	4.21	2.62	8.58	4.56	2656	(0.43, 0.55)
(Et-Cz–Tz)$_2$Ir(EO$_2$–pic)	14	3.64	5.62	3.63	9.42	5.17	2196	(0.43, 0.54)
(Et-Cz–Tz)$_2$Ir(pic-*N*-O)	14	3.34	3.64	2.40	7.72	4.25	2313	(0.43, 0.55)
(Et-Cz–Tz)$_2$Ir(EO$_2$–pic-*N*-O)	14	3.54	4.39	1.84	9.15	4.87	2915	(0.43, 0.56)

[a] At 1 cd m^{-2}. [b] Maximum efficiency. [c] Values collected at a current density of 100 mA cm^{-2}. [d] Values collected at a current density of 10 mA cm^{-2}.

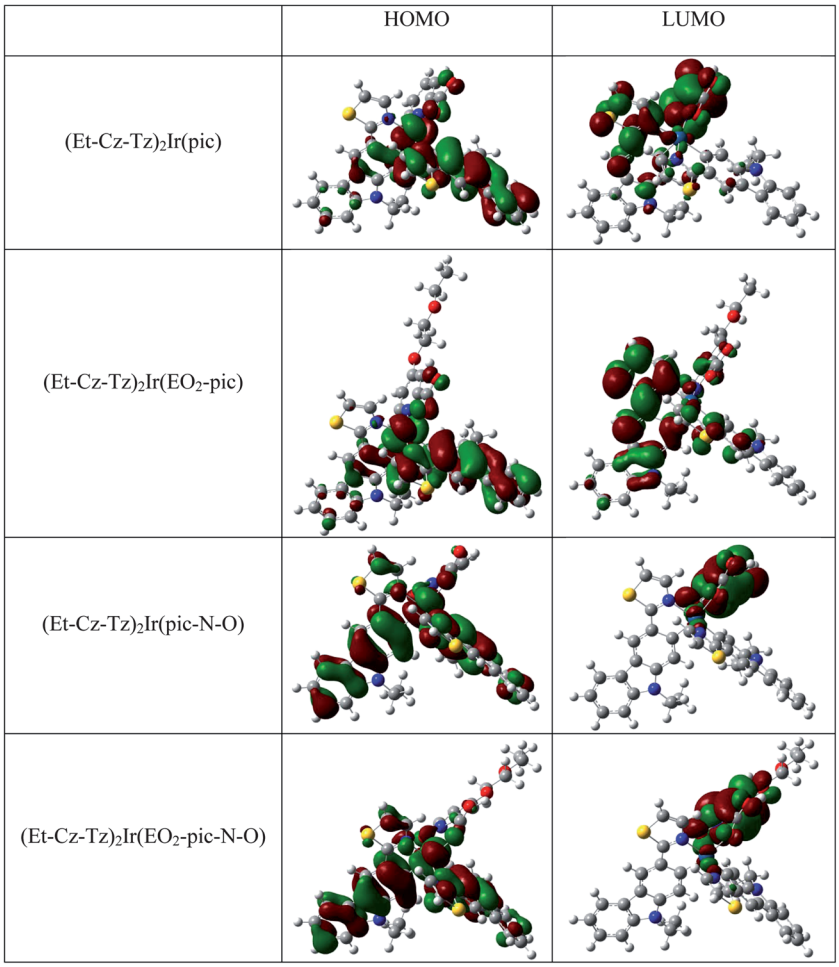

Fig. 9 Calculated HOMOs and LUMOs of Ir(III) complexes.

4.013, 4.001, 3.916, and 3.894 eV, respectively, which corresponds to the absorption wavelengths of 308.93, 309.95, 316.80, and 318.43 nm. These values closely correlate with the respective experimentally determined absorption wavelengths of 322, 322, 324, and 323 nm.

Conclusions

The investigation described above has led to the design and first synthesis of novel, solution processable heteroleptic Ir(III) complexes using a tandem reaction. Evaluations of the performances of the solution processable PhOLEDs, comprised of these Ir(III) complexes, demonstrated that they display high brightness levels, EQE and luminance efficiencies of 2450 cd m^{-2}, 6.89% and 10.98 cd A^{-1}, with CIE coordinates of (0.44, 0.54). The combination of high efficiency and solution processability of PhOLEDs that employ these Ir(III) complexes makes them promising candidates for use in light emitting diode devices.

Experimental

General information

All chemicals and reagents were purchased from Aldrich Chemical Co. and used without further purification. THF was dried and purified by distillation over sodium/benzophenone under a N_2 atmosphere, and other solvents were used without purification. 3-Bromo-9-ethyl-9*H*-carbazole and 9-ethyl-3-(4,4,5,5-tetramethyl-1,3,2-dioxaborolan-2-yl)-9*H*-carbazole were synthesized using the procedure we have developed previously.[20] The ^{1}H- and ^{13}C-NMR spectra were recorded on a Varian Mercury Plus 300 and 600 MHz spectrometer in $CDCl_3$ using tetramethylsilane as the internal reference. The chemical shifts were reported in ppm relative to the singlet of $CDCl_3$ at 7.26 and 77 ppm for the ^{1}H- and ^{13}C-NMR, respectively. The infrared spectra were recorded at room temperature using a Perkin-Elmer Fourier Transform Infrared Spectrometer, Model spectra 100 series (Perkin-Elmer Corporation, Norwalk, CT, USA). High-resolution mass spectra data were obtained from the Korea Basic Science and Institute Daejeon Center (HR-ESI Mass). The UV-visible and fluorescence spectra were recorded with JASCO V-570 and Hitachi F-4500 fluorescence spectrophotometers at room temperature. Thermal analyses were carried out on a Mettler Toledo TGA/SDTA 851e, DSC 822e analyzer under an N_2 atmosphere at a heating rate of 10 °C min^{-1}. Cyclic voltammetry (CV) studies were carried out with a CHI 600C potentiostat (CH Instruments) at a scan rate of 100 mV s^{-1} in a 0.1 M solution of tetra-*n*-butylammonium hexafluorophosphate ($TBAPF_6$) in anhydrous acetonitrile–benzene (1 : 1.5 v/v). A platinum wire was used as the counter electrode

and an $Ag/AgNO_3$ electrode was used as the reference electrode. The potentials were referenced to the ferrocene/ferrocenium redox couple (Fc/Fc^+). It was assumed that the redox potential of Fc/Fc^+ had an absolute energy level of −4.8 eV to vacuum. The potential of Fc/Fc^+ was measured under the same conditions and located at 0.09 V relative to the Ag/Ag^+ electrode. All electrochemical experimental were carried out under an air atmosphere at room temperature.

Synthesis of 2-(9-ethyl-9*H*-carbazol-3-yl)thiazole (Et-Cz–Tz) (2)

9-Ethyl-3-(4,4,5,5-tetramethyl-1,3,2-dioxaborolan-2-yl)-9*H*-carbazole (**1**) (0.2 g, 0.62 mmol) was dissolved in THF (20 mL). Then, 2-bromothiazole (0.06 mL, 0.68 mmol), K_2CO_3 (0.6 mL, 4 M) and ethanol (0.4 mL) were added to the mixture, which was then stirred at 85 °C for 15 h under an N_2 atmosphere. After confirmation of the disappearance of (**1**) by using TLC, the solution was concentrated *in vacuo* giving an organic layer that was poured into water and extracted with diethyl ether. The combined organic layers were washed with brine, dried over anhydrous $MgSO_4$ and concentrated *in vacuo*, giving a residue that was subjected to column chromatography on silica gel using ethyl acetate–hexane–dichloromethane (1 : 7 : 2) as the eluent. The obtained product was further purified by recrystallization from methylene chloride : hexane to give a 2-(9-ethyl-9*H*-carbazol-3-yl)thiazole (Et-Cz–Tz) (0.13 g, 76%). Mp: 89–91 °C. ^{1}H NMR (300 MHz, $CDCl_3$): δ 8.77 (d, 1H), 8.17–8.21 (d, 1H), 8.06–8.21 (d, 1H), 7.90–7.91 (d, 1H), 7.47–7.50 (t, 1H), 7.25–7.37 (m, 4H), 4.23–4.25 (m, 2H), 1.35–1.40 (m, 2H); ^{13}C NMR (300 MHz, $CDCl_3$): δ 169.5, 130.0, 129.5, 126.1, 125.1, 124.8, 121.7, 121.3, 119.9, 119.1, 116.8, 116.2, 111.6, 109.6, 103.3, 40.3, 14.2.

Synthesis of 4-chloropicolinic acid-*N*-oxide (4)

A solution of 4-chloropicolinic acid (1 g, 6.34 mmol) and hydrogen peroxide (4.96 g, 146 mmol) in acetic acid (13 g, 44 mmol) was stirred for 12 h at 80 °C under a N_2 atmosphere. The solvent was removed by vacuum distillation and the residue was subjected to recrystallization using ethanol. The resulting product was obtained by sublimation to yield 4-chloropicolinic acid-*N*-oxide (0.29 g, 26%). ^{1}H NMR (300 MHz, CD_3OD): δ (ppm) 8.61–8.63 (d, 1H), 8.52–8.57 (d, 1H), 7.68–7.73 (m, 1H).

Synthesis of [2-(9-ethyl-9*H*-carbazol-3-yl)thiazole]iridium 4-(2-ethoxyethoxy)picolinic acid *N*-oxide (Et-Cz–Tz)$_2$Ir(EO$_2$–pic-*N*-O) *via* a tandem reaction

The cyclometalated Ir(III) μ-chloride bridged dimer, (Et-Cz–Tz)$_2$Ir(μ-Cl)Ir(Et-Cz–Tz)$_2$ (**3**), was synthesized using the method described by Nonoyama.[45] Et-Cz–Tz (**2**) (5 g, 18 mmol) and $IrCl_3 \cdot 3H_2O$ (2.9 g, 8.2 mmol) were added to a mixture of 2-ethoxyethanol and water (100 mL, 3 : 1 v/v). The resulting mixture was stirred at 140 °C for 20 h under a N_2 atmosphere, cooled to room temperature and the formed yellow solid was collected by filtration and washed with water and methanol. Subsequently, the solid was dried in a vacuum oven to afford a cyclometalated Ir(III) μ-chloride bridged dimer (**3**) as a yellow solid in 46% yield.

A solution of a cyclometalated Ir(III) μ-chloride bridged dimer (**3**) (2 g, 1.53 mmol), 4-chloropicolinic acid-*N*-oxide (1.33 g, 7.65 mmol) and Na_2CO_3 (1.6 g, 15.3 mmol) in 2-ethoxyethanol (30 mL) was stirred at reflux under a N_2 atmosphere for 12 h. After cooling to room temperature, the mixture was poured into water and extracted with ethyl acetate. The organic layer was dried over anhydrous $MgSO_4$ and concentrated *in vacuo*, giving a residue that was subjected to silica gel column chromatography using ethyl acetate : hexane (4 : 1) as the eluent. The obtained product was further purified by recrystallization from methylene chloride–hexane to give [2-(9-ethyl-9*H*-carbazol-3-yl)thiazole]iridium 4-(2-ethoxyethoxy)picolinic acid *N*-oxide [(Et-Cz–Tz)$_2$Ir(EO$_2$–pic-*N*-O)] (0.78 g, 58%) as a yellow solid. ^{1}H NMR (300 MHz, $CDCl_3$): δ (ppm) 8.31–8.33 (d, 1H), 8.23–8.26 (d, 2H), 7.83–7.94 (m, 5H), 7.12–7.29 (m, 11H), 4.20–4.22 (t, 2H), 3.97–4.02 (t, 4H), 3.75–3.76 (t, 2H), 3.53–3.56 (t, 2H), 1.14–1.21 (t, 9H); ^{13}C NMR (300 MHz, $CDCl_3$): δ (ppm) 169.2, 168.5, 158.5, 144.0, 140.0, 136.8, 126.3, 125.3, 124.7, 121.9, 121.7, 121.4, 119.7, 119.5, 118.7, 118.0, 111.3, 109.7, 103.3, 69.8, 69.3, 66.6, 40.2, 15.3, 14.5; anal. calcd for $C_{44}H_{38}IrN_5O_5S_2$: C, 54.31; H, 3.94; N, 7.20. Found: C, 54.46; H, 3.92; N, 7.22%. HRESI-MS $[M + H]^+$: *m*/*z* found 973.1924, calcd for 973.1910.

The above methodology with the cyclometalated Ir(III) μ-chloride bridged dimer (**3**) and the ancillary ligands picolinic acid, 4-chloropicolinic acid and picolinic acid *N*-oxide was used to prepare the other Ir(III) complexes: [2-(9-ethyl-9*H*-carbazol-3-yl)thiazole]iridium picolinic acid [(Et-Cz–Tz)$_2$Ir(pic)], [2-(9-ethyl-9*H*-carbazol-3-yl)thiazole]iridium 4-(2-ethoxyethoxy)picolinic acid [(Et-Cz–Tz)$_2$Ir(EO$_2$–pic)], and [2-(9-ethyl-9*H*-carbazol-3-yl)thiazole]iridium picolinic acid *N*-oxide [(Et-Cz–Tz)$_2$Ir(pic-*N*-O)], respectively.

(Et-Cz–Tz)$_2$Ir(pic). ^{1}H NMR (300 MHz, $CDCl_3$): δ (ppm): 8.32–8.35 (d, 1H), 8.25–8.28 (d, 2H), 7.88–7.99 (m, 5H), 7.07–7.37 (m, 11H), 6.75–6.76 (d, 1H), 3.98–4.04 (m, 4H), 1.19–1.24 (t, 6H): ^{13}C NMR (300 MHz, $CDCl_3$): δ (ppm) 174.2, 149.2, 148.3, 144.2, 137.9, 127.5, 126.5, 125.1, 124.7, 121.7, 121.5, 119.8, 119.6, 118.8, 118.1, 111.3, 109.6, 103.5, 40.3, 14.7; anal. calcd for $C_{40}H_{30}IrN_5O_2S_2$: C, 55.28; H, 3.48; N, 8.06. Found: C, 55.13; H, 3.49; N, 8.09%. HRESI-MS $[M + H]^+$: *m*/*z* found 869.1573, calcd for 869.1507.

(Et-Cz–Tz)$_2$Ir(EO$_2$–pic). ^{1}H NMR (300 MHz, $CDCl_3$): δ (ppm) 8.24–8.27 (d, 2H), 7.94–7.99 (m, 3H), 7.86–7.87 (d, 1H), 7.65–7.68 (d, 1H), 7.13–7.36 (m, 10H), 7.79–7.80 (m, 2H), 4.21–4.23 (t, 2H), 3.99–4.03 (t, 4H), 3.78–3.78 (t, 2H), 3.55–3.57 (t, 2H), 1.19–1.24 (t, 9H); ^{13}C NMR (300 MHz, $CDCl_3$): δ (ppm) 174.2, 168.3, 160.2, 150.1, 149.3, 144.2, 126.3, 125.2, 121.7, 121.5, 119.8, 119.5, 118.8, 118.0, 111.7, 111.6, 109.7, 109.4, 103.3, 69.8, 69.6, 66.5, 40.2, 15.4, 14.6; anal. calcd for $C_{44}H_{38}IrN_5O_4S_2$: C, 55.21; H, 4.00; N, 7.32. Found: C, 54.99; H, 4.01; N, 7.59%. HRESI-MS $[M + H]^+$: *m*/*z* found 957.2072, calcd for 957.1739.

(Et-Cz–Tz)$_2$Ir(pic-*N*-O). ^{1}H NMR (600 MHz, $CDCl_3$): δ (ppm) 8.33–8.31 (d, 1H), 8.26 (s, 1H), 8.23 (s, 1H), 7.98–7.97 (d, 1H), 7.95–7.93 (d, 1H), 7.92–7.91 (t, 2H), 7.88–7.85 (m, 1H), 7.34–7.31 (m, 2H), 7.30–7.27 (t, 2H), 7.21–7.20 (m, 2H), 7.18–7.16 (d, 1H), 7.12–7.10 (t, 1H), 7.08–7.06 (t, 1H), 6.74–6.73 (d, 1H), 6.29 (s, 1H), 6.21 (s, 1H), 4.02–3.95 (m, 4H), 1.21–1.17 (m, 6H); ^{13}C NMR (300 MHz, $CDCl_3$): δ (ppm) 169.4, 168.6, 149.5, 148.2,

144.3, 137.5, 127.6, 126.4, 125.3, 124.4, 121.8, 121.4, 119.8, 119.3, 118.6, 118.0, 111.3, 109.7, 103.2, 40.3, 14.7; anal. calcd for $C_{40}H_{30}IrN_5O_3S_2$: C, 54.28; H, 3.42; N, 7.91. Found: C, 54.32; H, 3.43; N, 7.61%. HRESI-MS $[M + H]^+$: *m*/*z* found 885.1469, calcd for 885.1359.

PhOLEDs fabrication and measurements

An indium tin oxide (ITO) glass substrate with a sheet resistance of 20 Ω per square was washed sequentially with a substrate cleaning detergent, deionized water, acetone, and isopropyl alcohol. Finally the ITO was treated in a UV-ozone chamber for 15 min. A layer of PEDOT:PSS (40 nm, CLEVIOS P VP CH 8000) was spin-coated onto the ITO substrate, which was then baked in air at 150 °C for 20 min. The emitting layer was then spin-coated onto the PEDOT:PSS coated substrate using a mixed solution of *m*-MTDATA and TPBI (weight ratio, 2 : 1, chlorobenzene) and doped with 12 wt% of Ir(III) complexes. All solutions used in the PhOLED fabrication were filtered with a 0.20 μm PTFE (hydrophobic) syringe filter. The emitting layer was then annealed at 80 °C for 30 min in a glove box. Finally, as a cathode consisting of TPBI (20 nm)/LiF (1 nm)/Al (100 nm), was thermal vapor deposited with effective area of 4 mm^2 at a pressure 5×10^{-6} Torr. The film thickness was measured using an α-Step IQ surface profiler (KLA Tencor, San Jose, CA). EL spectra and current density–voltage–luminance (*J*–*V*–*L*) characteristics of PhOLEDs were measured using a programmable Keithley model 236 power source and a spectra scan CS-1000 photometer, respectively.

Acknowledgements

This work was supported by a grant from the National Research Foundation of Korea (NRF) funded by the Ministry of Education, Science and Technology (MEST) of Korea (no. 2011-0028320). The work at SKKU was supported by a NRF grant funded by the Korea government (MEST) (no. 2007-0056343).

Notes and references

1 Y. Chi and P. T. Chou, *Chem. Soc. Rev.*, 2010, **39**, 638.
2 J. A. G. Williams, A. J. Wilkinson and V. L. Whittle, *Dalton Trans.*, 2008, 2081.
3 C. Wu, H. H. Chen, K. T. Wong and M. E. Thompson, *J. Am. Chem. Soc.*, 2010, **132**, 3133.
4 K. T. Kamtekar, A. P. Monkman and M. R. Bryce, *Adv. Mater.*, 2010, **22**, 572.
5 M. Buda, G. Kalyuzhny and A. J. Bard, *J. Am. Chem. Soc.*, 2002, **124**, 6090.
6 Y. L. Tung, S. W. Lee, Y. Chi, L. S. Chen, C. F. Shu, F. I. Wu, A. J. Carty, P. T. Chou, S. M. Peng and G. H. Lee, *Adv. Mater.*, 2005, **17**, 1059.
7 Y. L. Tung, L. S. Chen, Y. Chi, P. T. Chou, Y. M. Cheng, E. Y. Li, G. H. Lee, C. F. Shu, F. I. Wu and A. J. Carty, *Adv. Funct. Mater.*, 2006, **16**, 1615.
8 A. R. Hosseini, C. Y. Koh, J. D. Slinker, S. F. Torres, H. D. Abruña and G. G. Malliaras, *Chem. Mater.*, 2005, **17**, 6114.
9 Y. M. Cheng, G. H. Lee, P. T. Chou, L. S. Chen, Y. Chi, C. H. Yang, Y. H. Song, S. Y. Chang, P. I. Shih and C. F. Shu, *Adv. Funct. Mater.*, 2008, **18**, 183.
10 F. Huang, P. I. Shih, C. F. Shu, Y. Chi and A. K. Y. Jen, *Adv. Mater.*, 2009, **21**, 361.
11 Q. S. Zhang, Q. G. Zhou, Y. X. Cheng, L. X. Wang, D. G. Ma, X. B. Jing and F. S. Wang, *Adv. Funct. Mater.*, 2006, **16**, 1203.
12 T. H. Kwon, Y. H. Oh, I. S. Shin and J. I. Hong, *Adv. Funct. Mater.*, 2009, **19**, 711.
13 H. C. Su, F. C. Fang, T. Y. Hwu, H. H. Hsieh, H. F. Chen, G. H. Lee, S. M. Peng, K. T. Wong and C. C. Wu, *Adv. Funct. Mater.*, 2007, **17**, 1019.
14 S. Graber, K. Doyle, M. Neuburger, C. E. Housecroft, E. C. Constable, R. D. Costa, E. Ortí, D. Repetto and H. J. Bolink, *J. Am. Chem. Soc.*, 2008, **130**, 14944.
15 C. L. Ho, W. Y. Wong, Q. Wang, D. G. Ma, L. X. Wang and Z. Y. Lin, *Adv. Funct. Mater.*, 2008, **18**, 928.
16 H. Wu, J. Zou, F. Liu, L. Wang, A. Mikhailovsky, G. C. Bazan, W. Yang and Y. Cao, *Adv. Mater.*, 2008, **20**, 696.
17 H. Wu, G. Zhou, J. Zou, C. L. Ho, W. Y. Wong, W. Yang, J. Peng and Y. Cao, *Adv. Mater.*, 2009, **21**, 4181.
18 S. J. Lee, J. S. Park, M. S. Song, I. A. Shin, Y. I. Kim, J. W. Lee, J. W. Kang, Y. S. Gal, S. Kang, J. Y. Lee, S. H. Jung, H. S. Kim, M. Y. Chae and S. H. Jin, *Adv. Funct. Mater.*, 2009, **19**, 2205.
19 J. S. Park, M. K. Song, S. H. Jin, J. W. Lee, C. W. Lee and Y. S. Gal, *Macromol. Chem. Phys.*, 2009, **210**, 1572.
20 Y. Tao, Q. Wang, C. Yang, Q. Wang, Z. Zhang, T. Zou, J. Qin and D. G. Ma, *Angew. Chem., Int. Ed.*, 2008, **47**, 8104.
21 S. Bettington, M. Tavasli, M. R. Bryce, A. Beeby, H. Al-Attar and A. P. Monkman, *Chem.–Eur. J.*, 2007, **13**, 1423.
22 J. K. Politis, M. D. Curtis, Y. He and J. Kanichki, *Macromolecules*, 1999, **32**, 2484.
23 J. K. Politis, M. D. Curtis, L. Gonzalez, D. C. Martin, Y. He and J. Kanicki, *Chem. Mater.*, 1998, **10**, 1713.
24 J. Lee, B. J. Jung, S. K. Lee, J. I. Lee, H. J. Cho and H. K. Shim, *J. Polym. Sci., Part A: Polym. Chem.*, 2005, **43**, 1845.
25 C. Yang, X. Zhang, H. You, L. Zhu, L. Chen, L. Zhu, Y. Tao, D. Ma, Z. Shuai and J. Qin, *Adv. Funct. Mater.*, 2007, **17**, 651.
26 T. L. Ho, *Tandem Organic Reactions*, Wiley, New York, 1992.
27 K. C. Nicolaou, D. J. Edmonds and P. G. Bulger, *Angew. Chem., Int. Ed.*, 2006, **45**, 7134.
28 R. N. Bera, N. Cumpstey, P. L. Burn and I. D. W. Samuel, *Adv. Funct. Mater.*, 2007, **17**, 1149.
29 S. Feng, L. Duan, L. Hou, J. Qiao, D. Zhang, G. Dong, L. Wang and Y. Qiu, *J. Phys. Chem. C*, 2011, **115**, 14278.
30 Y. Shirota, *J. Mater. Chem.*, 2005, **15**, 75.
31 M. Long, M. L. Boroson, D. R. Freeman, B. E. Koppe, T. W. Palone and N. P. Redden, *Dig. Tech. Pap. - Soc. Inf. Disp. Int. Symp.*, 2008, **39**, 507.
32 H. Yang, F. I. Wu, D. Neher, C. H. Chien and C. F. Shu, *Chem. Mater.*, 2008, **20**, 1629.
33 Y. J. Pu, M. Higashidate, K. I. Nakayama and J. Kido, *J. Mater. Chem.*, 2008, **18**, 4183.
34 J. Ding, J. Lü, Y. Cheng, Z. Xie, L. Wang, X. Jing and F. S. Wang, *Adv. Funct. Mater.*, 2008, **18**, 2754.
35 B. Liang, L. Wang, Y. Xu, H. Shi and Y. Cao, *Adv. Funct. Mater.*, 2007, **17**, 3580.

36 C. L. Ho, W. Y. Wong, G. J. Zhou, Z. Xie and L. Wang, *Adv. Funct. Mater.*, 2007, **17**, 2925.
37 S. C. Lo, C. P. Shipley, R. N. Bera, R. E. Harding, A. R. Cowley, P. L. Burn and I. D. W. Samuel, *Chem. Mater.*, 2006, **18**, 5119.
38 P. J. Hay, *J. Phys. Chem. A*, 2002, **106**, 1634.
39 M. C. Columbo, A. Hauser and H. U. Güdel, *Top. Curr. Chem.*, 1994, **171**, 143.
40 Y. Wang, N. Herron, V. V. Grushin, D. LeCloux and V. Petrov, *Appl. Phys. Lett.*, 2001, **79**, 449.
41 K. Suzuki, A. Endo, T. Yoshihara, S. Tobita, M. Yahiro, D. Yokoyama and C. Aadachi, *Proc. SPIE–Int. Soc. Opt. Eng.*, 2009, **7415**, 741504.
42 K. A. King, P. J. Spellane and R. J. Watts, *J. Am. Chem. Soc.*, 1985, **107**, 1431.
43 s. Reineke, k. Walzer and K. Leo, *Phys. Rev. B: Condens. Matter Mater. Phys.*, 2007, **75**, 125328.
44 M. J. Frisch, G. W. Trucks, H. B. Schlegel, G. E. Scuseria, M. A. Robb, J. R. Cheeseman, G. Scalmani, V. Barone, B. Mennucci, G. A. Petersson, H. Nakatsuji, M. Caricato, X. Li, H. P. Hratchian, A. F. Izmaylov, J. Bloino, G. Zheng, J. L. Sonnenberg, M. Hada, M. Ehara, K. Toyota, R. Fukuda, J. Hasegawa, M. Ishida, T. Nakajima, Y. Honda, O. Kitao, H. Nakai, T. Vreven, J. A. Montgomery, Jr, J. E. Peralta, F. Ogliaro, M. Bearpark, J. J. Heyd, E. Brothers, K. N. Kudin, V. N. Staroverov, R. Kobayashi, J. Normand, K. Raghavachari, A. Rendell, J. C. Burant, S. S. Iyengar, J. Tomasi, M. Cossi, N. Rega, J. M. Millam, M. Klene, J. E. Knox, J. B. Cross, V. Bakken, C. Adamo, J. Jaramillo, R. Gomperts, R. E. Stratmann, O. Yazyev, A. J. Austin, R. Cammi, C. Pomelli, J. W. Ochterski, R. L. Martin, K. Morokuma, V. G. Zakrzewski, G. A. Voth, P. Salvador, J. J. Dannenberg, S. Dapprich, A. D. Daniels, Ö. Farkas, J. B. Foresman, J. V. Ortiz, J. Cioslowski and D. J. Fox, *Gaussian 09, Revision A.1*, Gaussian, Inc., Wallingford, CT, 2009.
45 M. Nonoyama, *J. Organomet. Chem.*, 1975, **86**, 263.

